Alpha particle cluster states in fp-shell nuclei

A. C. Merchant
Instituto de Estudos Avançados, Centro Técnico Aeroespacial, 12.200 São José dos Campos, São Paulo, Brazil
(Received 16 March 1987)

Alpha particle cluster structure is known experimentally to persist throughout the mass range $16 \leq A \leq 20$, and has been very successfully described in this region in terms of the Buck-Dover-Vary local potential cluster model. It is argued that an analogous cluster structure should be present in nuclei at the beginning of the fp shell, and the available experimental data are examined to determine likely alpha particle cluster state candidates in the mass range $40 \leq A \leq 44$. Calculations of the cluster state spectra and mean square cluster-core separation distances (which may be readily used to evaluate $E2$ electromagnetic transition rates) for ^{40}Ca, ^{42}Ca, ^{42}Sc, ^{43}Sc, ^{43}Ti, and ^{44}Ti using the above-mentioned model are presented, and compared with experimental measurements where possible. The agreement between theory and experiment is generally good (although inferior to that obtained in the sd shell), and points to the desirability of an extension and improvement of the measurements of the properties of the excited states in these nuclei.

I. INTRODUCTION

It is now well established that alpha particle cluster structure is present in many light nuclei (Ref. 1) (having mass numbers $A \leq 40$). More recently, it has been suggested that alpha cluster states may also be present in rare earth (Ref. 2) and actinide (Ref. 3) nuclei, indicating that their occurrence could well be a stable feature across a large part of the periodic table.

Among the lighter nuclei, very similar alpha cluster structure is observed not only in ^{16}O and ^{20}Ne, but also found to persist across the neighboring nuclei ^{18}O, ^{18}F, ^{19}F, and ^{19}Ne (Refs. 4–10) in a basically unchanged form, except for some modifications due to the different spins involved in the various cluster-core combinations. Since the beginning of the fp shell is in many ways analogous to the beginning of the sd shell, this observation strongly suggests that very similar alpha cluster states may also be present in ^{40}Ca, ^{44}Ti, and across the neighbors ^{42}Ca, ^{42}Sc, ^{43}Sc, and ^{43}Ti. Indeed, a few nuclei in this mass region have recently received a good deal of theoretical attention in terms of cluster models (Refs. 11–15). In particular, a subset of the excited states of ^{40}Ca and ^{44}Ti show the classical signatures of ^{36}Ar-α and ^{40}Ca-α cluster-core structure, namely strong, selective excitation in alpha particle transfer reactions onto the appropriate target, "rotational" energy spectra [varying like $L(L+1)$], and enhanced $E2$ electromagnetic transition rates (Refs. 16–19). Unfortunately, there appear to be no measurements of alpha decay widths for these states, which might provide an even more conclusive proof of their alpha cluster structure.

In this paper we shall examine the available experimental data for these fp-shell nuclei and present calculations employing the Buck-Dover-Vary local potential cluster model (Ref. 4) for comparison. This model has the advantage of giving an intuitively appealing picture of the cluster-core system and involves relatively simple calculations, as opposed to a full coupled-channel resonating group model treatment (Ref. 20), which for nuclei as heavy as this would be prohibitively complicated. In this way we can investigate the question of the persistence of alpha clustering across the neighboring nuclei in the mass range $40 \leq A \leq 44$, so as to confirm that it is a stable feature in this area of the periodic table.

II. THE BUCK-DOVER-VARY CLUSTER MODEL

The original single channel form of the model describes the central part of the interaction between an alpha particle cluster and the remaining core nucleons by means of a local potential which is obtained by folding the densities of the two constituents with an effective nucleon-nucleon potential. This local potential can be conveniently and accurately parametrized in the form

$$V(r)=\frac{-V_0[1+\cosh(R/a)]}{\cosh(r/a)+\cosh(R/a)}\ , \tag{2.1}$$

where the radius parameter R and the diffuseness parameter a define the geometry of the potential, and the depth V_0 can be fine tuned so that the model reproduces the experimental value of the cluster-core separation energy. Pal and Lovas (Ref. 12) used $R=2.9$ fm and $a=1.4$ fm for the ^{36}Ar-α system and $R=3.0$ fm and $a=1.4$ fm for ^{40}Ca-α, and we shall endeavor to use very similar parameter values in the following to describe the intermediate cluster-core combinations, since such similar components in the folding integral are clearly expected to give rise to very similar central potentials.

Both cluster and core are treated as inert, structureless entities whose relative motion can be characterized by the principal quantum number N and the orbital angular momentum L. However, these quantum numbers are restricted to correspond to the microscopic situation in which the cluster nucleons are completely excluded from the last major shell occupied by the core nucleons. In the

present study, where the alpha particle cluster nucleons will be placed in the *fp* shell, this constraint will be written as

$$N = 2n + L \geq 12 \ . \tag{2.2}$$

(where n is the number of interior nodes in the radial wave function). In this way the main requirements of the Pauli exclusion principle are satisfied, and any remaining effects of antisymmetrization may be incorporated into the effective potential of Eq. (2.1).

The cluster state energies and wave functions are then identified as the bound states and resonances obtained by solving the single-particle Schrödinger equation for the above mentioned parametrization of the folded potential (plus Coulomb and centrifugal terms as appropriate), and their properties computed for comparison with the available experimental data. The cluster-core Coulomb potential is taken to be that appropriate to a point charge (the cluster) interacting with a uniformly charged sphere (the core) of radius R_c ($R_c = 4.0$–4.1 fm in the cases of interest that follow).

III. PHENOMENOLOGY

The lowest lying alpha particle cluster states in the nuclei at the beginning of the *sd* shell are experimentally well established on the basis of strong selective excitation in alpha particle transfer reactions, "rotationally" spaced energies, enhanced $E2$ electromagnetic transitions between band members (usually tens of Weisskopf units), and, in the cases of those states above the cluster-core separation threshold, large alpha decay widths (several times the Wigner single particle limit). They have been very satisfactorily described within the framework of the Buck-Dover-Vary cluster model (Refs. 4–10) and their spectra are displayed in the lower panel of Fig. 1.

The regular "rotational" energy spacings of the cluster states are readily seen to be a common feature persisting from one nucleus to another and the effects of noncentral forces in the $^{14}N-\alpha=^{18}F$ and $^{15}N-\alpha=^{19}F$ systems are apparent. In these latter cases the cores, in their ground states, have spin-parity values of 1^+ and $\frac{1}{2}^-$, respectively, which give rise to tensor and/or spin-orbit forces between cluster and core. These, in turn, lift the degeneracy of the triplets (spin-1 core) or doublets (spin-$\frac{1}{2}$ core) of the "rotational" levels, but leave the basic structure intact, acting essentially as a perturbation on the central part of the cluster-core potential. A summary of the experimental information available for these nuclei can be found in Refs. 21 and 22.

The experimental situation relating to the nuclei at the beginning of the *fp* shell is not so clear cut. Alpha transfer reactions have been performed to populate states in ^{40}Ca and ^{44}Ti (Refs. 16–18), so that their alpha cluster state candidates can be readily assigned, but the intermediate nuclei are essentially inaccessible to this type of experiment (requiring difficult or even impossible targets of ^{38}Ar, ^{38}K, ^{39}K, and ^{39}Ca). Even the gamma ray spectroscopy of ^{42}Ca, ^{42}Sc, ^{43}Sc, and ^{43}Ti has not been vigorously pursued, and spin-parity values are not very thoroughly documented for states with excitation energies above about 2 MeV (see, for example, Ref. 19). Nevertheless, on the basis of those available spin-parity assignments and electromagnetic transition rates, some ten states in ^{43}Sc, and their partners in the mirror nucleus ^{43}Ti, can be nominated as having a predominantly $^{39}K/^{39}Ca(g.s.)+\alpha$ structure (Ref. 13). In ^{42}Ca and ^{42}Sc the available experimental information is even more meager, and further measurements to determine their spectra would be most welcome.

As an additional aid to the identification of alpha cluster states in these nuclei, recourse may be taken to shell model calculations. McGrory (Ref. 23) has systematically investigated the nuclei at the beginning of the *fp* shell, using a modified version of the Kuo-Brown interaction. Although he obtains good agreement with experiment for many states, corresponding to the simpler configurations, there are also several known states which are not so well reproduced. Since we expect a truncated shell model calculation to have difficulties in building up the spatial correlations among the active nucleons necessary to describe an alpha particle cluster configuration, such disagreements may be taken as possible indicators of the

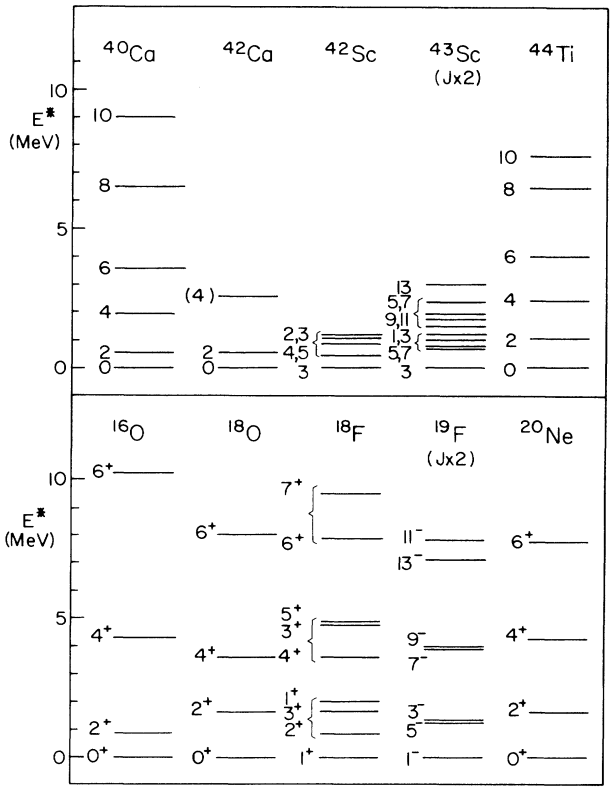

FIG. 1. Upper panel: the experimentally determined energies and spins of the proposed alpha particle cluster states in nuclei at the beginning of the *fp* shell. All these states have positive parity. Lower panel: the experimentally determined energies and spin-parity values of the well established alpha particle cluster states in nuclei at the beginning of the *sd*-shell. This frame is an extended version of a similar figure in Ref. 5. All energies are given relative to the lowest lying cluster state of the given nucleus, which is not necessarily the ground state.

states we desire. Since these considerations agree with the nomination of the better established alpha cluster states in ^{43}Sc/^{43}Ti and ^{44}Ti, we use them here to assist in the identification of the less well known cluster states in ^{42}Ca and ^{42}Sc.

The upper panel of Fig. 1 summarizes the present experimental situation with respect to alpha cluster states in the nuclei at the beginning of the *fp* shell. There are clearly a lot of states expected by analogy with the spectra at the beginning of the *sd* shell, but which have not yet been found. Even so, we conclude that there are good indications of similar "rotational" behavior in the various nuclei, since the proposed bands of states are seen to be accounted for by a more or less common rotational parameter (or equivalently, moment of inertia).

The ground state ^{38}K core associated with ^{42}Sc has a spin-parity value of 3^+, while the ^{39}K core for ^{43}Sc has a value of $\frac{3}{2}^+$. The noncentral forces resulting from these spins are seen to weakly break the degeneracy of the rotational centroids in a slightly more complicated manner than in the *sd*-shell nuclei. However, the basic conclusion, that the "rotational" behavior due to the central part of the cluster-core interaction persists throughout all the nuclei considered, remains unchanged.

IV. CALCULATIONS FOR INDIVIDUAL NUCLEI

In this section we briefly review the Buck-Dover-Vary cluster model calculations for ^{40}Ca, ^{43}Sc/^{43}Ti, and ^{44}Ti that have already appeared in the literature (Refs. 11, 12, 13, and 15) and present original calculations for ^{42}Ca and ^{42}Sc. The central part of the effective cluster-core potential is very similar for all the nuclei studied. The noncentral forces present in those cases where the core has an intrinsic angular momentum (^{38}K + α and ^{39}K/^{39}Ca + α) are calculated semimicroscopically and found to be small. The results of a single channel calculation for the energies of the L centroids of the members of the $N=12$ bands in all the nuclei considered are shown in Table I, and the matrix elements of r^2 (the cluster-core separation distance) in Table II. These latter values can be used to calculate the mean square radii of the cluster states and also the $E2$ electromagnetic transition rates between them.

A. ^{40}Ca=^{36}Ar+α

The Buck-Dover-Vary cluster model was first applied to the ^{40}Ca=^{36}Ar + α system by Pal and Lovas (Ref. 12). They were able to identify the best experimental candidates for cluster structure because of their selective excitation in the ^{36}Ar(^{16}O,^{12}C)^{40}Ca transfer reaction (Ref. 18), and successfully calculated the energies of six members of the $N=12$ band (having $J^\pi=0^+,2^+,4^+,6^+,8^+,10^+$) as well as three enhanced $E2$ transitions ($6^+\rightarrow4^+$, $4^+\rightarrow2^+$, and $2^+\rightarrow0^+$) without the need to introduce effective charges. The $J^\pi=12^+$ member, which terminates the band, has not been seen experimentally.

The single channel form of the Buck-Dover-Vary cluster model has recently been extended to include excited states of the core in a coupled-channels formalism. This extension has been used to calculate the alpha cluster states in ^{40}Ca based on the ^{36}Ar core in its 0^+ ground state and 2^+ first excited state (assuming that these states are the first two members of a $K^\pi=0^+$ rotational band) (Ref. 15). Many more cluster states are predicted in ^{40}Ca, of which six have good experimental counterparts [$2^+(5.63)$, $3^+(6.03)$, $4^+(6.54)$, $2^+(6.91)$, $0^+(7.70)$, and $4^+(7.93)$] and an additional five $E2$ transition rates are calculated in close quantitative agreement with experiment (there are not more because of the lack of experimental data). The $E2$ transition strengths are strong when the cluster states between which the transition takes place are based on the same core state (tens of Weisskopf units) and much weaker when they are based on different core states (1 or 2 Weisskopf units). We conclude that the use of the model is well vindicated in this case, and confidently expect that further experimental investigations will locate the remaining predicted states.

B. ^{43}Sc/^{43}Ti=^{39}K/^{39}Ca+α

A calculation of the low lying alpha particle cluster states in ^{43}Sc (and thus equivalently of the $T=\frac{1}{2}$ isobaric

TABLE I. Calculated excitation energies of the centroids of the $N=12$ bands of alpha particle cluster states in the low *fp*-shell nuclei. V_0 is the depth of the potential of Eq. (2.1) chosen so as to reproduce the experimental cluster-core separation energy. $R=2.9$ fm and $a=1.4$ fm in all cases.

	Nucleus				
	^{40}Ca	^{42}Ca	^{42}Sc	^{43}Sc/^{43}Ti	^{44}Ti
			V_0 (MeV)		
	159.3	161.1	160.3	163.6	166.8
J^π of centroid	Excitation energies (MeV)				
0^+	3.34	1.83	2.18	0.15	0.00
2^+	3.87	2.36	2.71	0.68	0.53
4^+	5.12	3.61	3.96	1.93	1.78
6^+	7.14	5.62	5.97	3.93	3.78
8^+	9.99	8.45	8.80	6.76	6.60
10^+	13.77	12.21	12.58	10.51	10.35
12^+	18.69	17.09	17.47	15.37	15.18

TABLE II. Calculated values of $\langle L \mid r^2 \mid L' \rangle$ between the centroid states of the $N=12$ bands of alpha particle cluster states in the low fp-shell nuclei.

		Nucleus				
		^{40}Ca	^{42}Ca	^{42}Sc	^{43}Sc/^{43}Ti	^{44}Ti
L (of centroid)	L'	Calculated values of $\langle L \mid r^2 \mid L' \rangle$ (fm)^2				
0	0	29.15	28.25	28.83	27.60	26.77
2	2	28.98	28.08	28.66	27.42	26.60
4	4	28.54	27.64	28.22	26.98	26.16
6	6	27.79	26.89	27.47	26.23	25.42
8	8	26.65	25.74	26.33	25.10	24.30
10	10	24.93	24.05	24.62	23.44	22.69
12	12	22.31	21.56	22.04	21.05	20.43
0	2	29.00	28.10	28.69	27.45	26.62
2	4	28.41	27.50	28.09	26.85	26.02
4	6	27.27	26.35	26.94	25.69	24.87
6	8	25.42	24.49	25.09	23.83	23.01
8	10	22.50	21.57	22.17	20.93	20.14
10	12	17.49	16.66	17.20	16.10	15.42

analog states in ^{43}Ti) using the Buck-Dover-Vary cluster model has already appeared in the literature (Ref. 13). There are no reported alpha transfer data available for these nuclei and so the experimental cluster state candidates had to be identified from their spectroscopy and electromagnetic properties. The members of the $N=12$ band are expected to have a leading $(fp)^4(sd)^{-1}$ configuration in a shell model expansion (and positive parity). In this way experimental counterparts were found for 16 of the predicted states and nine $E2$ transitions were calculated in good agreement with the measured strengths.

The calculation treated the ground state of the ^{39}K core as a $d_{3/2}$ hole in the doubly closed shell nucleus ^{40}Ca, and also included the possibility of having an excited core in its first $\frac{1}{2}^+$ state (treated as an $s_{1/2}$ hole in ^{40}Ca). All the possible noncentral forces (spin-orbit as well as second and third rank tensor contractions) were calculated semimicroscopically (by a full application of the method illustrated in Sec. 4 of Ref. 8) and all except the tensor force of Eq. (4.1) below were found to be negligibly small,

$$V_T = V_2(r)[(\mathbf{S}\cdot\hat{\mathbf{r}})^2 - \tfrac{1}{3}S^2] \ , \tag{4.1}$$

where $\mathbf{S}$ is the core spin, $\hat{\mathbf{r}}$ the unit vector directed from the center of the core to the center of the cluster, and $V_2(r)$ is a radial form factor. Many predicted higher lying states (above ~ 3 MeV) remain without experimental counterparts since the gamma ray spectroscopy at these energies is very incomplete.

The results of a simplified single channel calculation are shown in Tables I and II. The energies of the L centroids of the $N=12$ band for a cosh potential [Eq. (2.1)] with the same geometry as the previous examples and a depth of $V_0=163.6$ MeV, and the matrix elements of r^2, are presented to emphasize the systematic variation of these quantities as one progresses across the shell from $A=40$ towards $A=44$. The rotational parameter (inverse moment of inertia) in this case is comparable with that of the other systems and the expectation values of r^2 exhibit a slight ($\sim 5\%$) reduction as compared with ^{40}Ca.

C. ^{44}Ti=^{40}Ca+α

The alpha particle cluster state spectrum in ^{44}Ti has been treated using the single channel version of the Buck-Dover-Vary cluster model by Pilt (Ref. 11) and by Pal and Lovas (Ref. 12). They both identify the members of the yrast band as the $N=12$ band of alpha cluster states, and are supported in this by the results of alpha transfer reactions (Refs. 16 and 17). Although Pilt reproduces the state energies better, the price he pays for this is an unphysically deep central potential (~ 400 MeV) and an overly small average cluster-core separation, which is reflected in unacceptably small $E2$ transition rates. Pal and Lovas reproduce the energies of the first five states (0^+, 2^+, 4^+, 6^+, and 8^+) well (but not the 10^+ and 12^+) and, in addition, calculate the six $E2$ transitions between the seven band members in fairly good agreement with experiment (and without introducing effective charges).

The results presented in Tables I and II are very similar to those of Pal and Lovas, except that we have maintained the same cosh potential geometry as in all the preceding subsections and chosen a depth of $V_0=166.8$ MeV to fit the binding energy of ^{44}Ti (they use $R=3.0$ fm, $a=1.4$ fm, and $V_0=161.9$ MeV).

A recent, more microscopic calculation (Ref. 15) has also addressed this cluster state spectrum and gives energies essentially in agreement with our own, and has the advantage of not treating the depth V_0 as a free parameter. In addition, the root mean square cluster-core separations of Ref. 15 show the same centrifugal antistretching effect (reduction with increasing L) as our own, but are systematically about 15% smaller. Like the authors of Ref. 15, we predict $N=13$ negative parity bands commencing some 5–6 MeV above the $N=12$ bandheads, in all the nuclei considered up to now, but in view of the complete absence of experimental data, do not press the

point here. However, we can conclude that the Buck-Dover-Vary cluster model works satisfactorily in ^{44}Ti.

D. ^{42}Ca=^{38}Ar+α

No cluster model calculations have previously been performed for the $^{42}Ca=^{38}Ar+\alpha$ system nor for the isospin-1 analog states in $^{42}Sc=^{38}K^*+\alpha$ and $^{42}Ti=^{28}Ca+\alpha$. Nor are any alpha transfer data available because of the difficulty (or even impossibility) of preparing the requisite targets. The only way, at present, to identify alpha cluster states in this nucleus is to note that we expect the bandhead to be low lying (0–3 MeV above the ground state by analogy with neighboring nuclei) and to select those states in this energy region which are badly reproduced in shell model calculations. From Table II of Ref. 23 we therefore tentatively select $T=1$ states $0^+(1.83)$ and $2^+(2.48)$, which are known to be connected by a strong $E2$ transition, and, from the compilation of Endt and van der Leun (Ref. 19), the $4^+(4.43)$. The upper panel of Fig. 1 shows that these states have energy differences similar to the alpha cluster states in ^{40}Ca (although the 4^+ is very speculative). The calculation of the energies for the entire $N=12$ band is presented in Table I using the same geometry [$R=2.9$ fm and $a=1.4$ fm in Eq. (2.1)] as for $^{40}Ca=^{36}Ar+\alpha$, and a depth of $V_0=161.1$ MeV to place the 0^+ bandhead at 1.83 MeV. Improved spectroscopy of the $T=1$ states in ^{42}Ca, ^{42}Sc, and ^{42}Ti would be very welcome to compare with these predictions, and Table II can be used to compare our predictions with future measurements of $E2$ transition rates.

E. ^{42}Sc=^{38}K+α

No previous Buck-Dover-Vary cluster model calculations of the $T=0$ states with $^{42}Sc=^{38}K+\alpha$ structure have been performed, and no alpha transfer reactions on ^{38}K targets have been reported. Since the proposed ^{38}K ground state core has spin parity 3^+, we expect a rather complicated spectrum of alpha particle cluster states in ^{42}Sc whose spins J are formed by coupling the cluster-core orbital angular momentum L with the core spin $S=3$ (i.e., $J=L\otimes S$). This will give rise to a low lying 3^+ cluster state (with $L=0$), followed by a quintuplet (based on $L=2$) and a series of higher lying septuplets corresponding to the larger values of L. The spectroscopy of ^{42}Sc is not complete enough to identify many of these states, but with the help of McGrory's shell model calculation (Ref. 23), and the cluster state spectra of the neighboring nuclei, we tentatively propose the $3^+(2.18)$ as the $L=0$ cluster state and the $4^+(2.35$ or $2.65)$, $5^+(3.09)$, $3^+(3.31)$, and $2^+(3.39)$ as four of the members of the $L=2$ quintuplet. From the upper panel of Fig. 1 we can see that this choice falls in with the systematics at the beginning of the fp shell and thus will allow us to choose V_0 to fit the energy of the bandhead and hence perform a Buck-Dover-Vary cluster model calculation for this system.

The energies which result from solving the Schrödinger equation with the potential of Eq. (2.1) (using $R=2.9$ fm, $a=1.4$ fm, and $V_0=160.3$ MeV) for the $N=12$ band of ^{38}K-α cluster states in ^{42}Sc are shown in Table I. Since the ^{38}K core carries a spin of 3 there are many types of noncentral forces which could be present in the cluster-core potential. However, experience in the sd shell teaches us that the most important of them will be the tensor force associated with the quadrupole deformation of the core. This can be written as in Eq. (4.1), and we shall now calculate the radial form factor $V_2(r)$ semimicroscopically.

A detailed example of the calculation of spin-orbit and tensor forces between a ^{14}N core and an alpha particle cluster is given in Ref. 8. The basic idea is to sum an alpha-nucleon interaction (which fits the low energy scattering data) over the nucleons in the core. To calculate $V_2(r)$ for a ^{14}N core, this is equivalent to summing the alpha-nucleon interaction over two p-shell holes coupled to spin 1 in ^{16}O, and for the ^{38}K core of interest here, it will be equivalent to summing over two sd-shell holes in ^{40}Ca. Although the alpha-nucleon potential contains both central and spin-orbit terms, the former is very much more important in the calculation of $V_2(r)$ (because the central potential is much deeper than the spin-orbit potential) and we shall consider only the central term here for simplicity.

To begin with, we need a description of the ground state of the ^{38}K core. In treating this as two sd-shell holes in ^{40}Ca coupled to spin 3, we have, in principle, four possible combinations, $(d_{3/2})^{-2}$, $(d_{5/2}^{-1},s_{1/2}^{-1})$, $(d_{3/2}^{-1},d_{5/2}^{-1})$, and $(d_{5/2})^{-2}$, To simplify the ensuing algebra, we shall, however, assume that the ground state is well described by the single configuration $(d_{3/2})^{-2}$. Making a tensor decomposition of the central part of the alpha-nucleon potential, retaining only the quadrupole term, and following the same steps as in Sec. 4 of Ref. 8, much simplified by setting all hole angular momenta equal to $\frac{3}{2}$, we arrive at the following expression for the radial form factor $V_2(r)$,

$$V_2(r)=\tfrac{2}{5}F_2^{22}(r)\ , \tag{4.2}$$

where, in general, $F_2^{ll'}(r)$ is given by

$$F_2^{ll'}(r)=\int_0^\infty U_2(x,r)\mathcal{R}_l^*(x)\mathcal{R}_{l'}(x)x^2dx\ , \tag{4.3}$$

with $R_l(x)$ being a radial wave function for an sd-shell hole of orbital angular momentum l, and $U_2(x,r)$ the quadrupole term in the tensor decomposition of the alpha-nucleon central potential, $U(|\mathbf{x}-\mathbf{r}|)$, namely

$$U_2(x,r)=\tfrac{1}{2}\int_{-1}^{1}U(|\mathbf{x}-\mathbf{r}|)P_2(\cos\theta)d(\cos\theta)\ . \tag{4.4}$$

If we choose oscillator radial wave functions for $\mathcal{R}_l(x)$ and a Gaussian alpha-nucleon potential such as that of Batty *et al.* (Ref. 24), the integrals of Eqs. (4.3) and (4.4) can be evaluated analytically. We therefore write

$$\mathcal{R}_2(x)=\left[\frac{16}{15b^3\sqrt{\pi}}\right]^{1/2}\frac{x^2}{b^2}e^{-(x^2/2b^2)}\ , \tag{4.5}$$

and we find that

$$F_2^{22}(r)=\frac{a^3b^2U_0}{(a^2+b^2)^{9/2}}\frac{2r^2}{15}\left[7a^2+\frac{2b^2r^2}{a^2+b^2}\right]e^{-r^2/(a^2+b^2)}\ . \tag{4.6}$$

The resulting form factor $V_2(r)$ is shown in the upper

panel of Fig. 2 for an alpha-nucleon potential having depth $U_0 = -43.0$ MeV and range $a = 1.90$ fm, while an oscillator length parameter $b = 1.87$ fm is used to represent the *sd*-shell holes.

It is now possible to calculate the splittings of the degenerate L centroids of the $^{42}\mathrm{Sc} = {}^{38}\mathrm{K} + \alpha$ cluster-core spectrum due to the tensor force of Eq. (4.1). For the energy $E(J,L)$ of a state of total angular momentum J $(= L \otimes S)$, the model gives (with $S = 3$)

$$E(J,L) = E_0(L) - \frac{[A(A+1) - 16L(L+1)]}{2(2L-1)(2L+3)} \gamma_L \ , \qquad (4.7)$$

where $E_0(L)$ is the energy of the L centroid (see Table I) and

$$A = J(J+1) - L(L+1) - 12 \ , \qquad (4.8)$$

and we are ignoring the effects of the off-diagonal matrix elements of the tensor force. The parameter γ_L is defined by

$$\gamma_L = \int_0^\infty V_2(r) \, | \, \chi_L(r) \, | \, ^2 dr \ . \qquad (4.9)$$

The cluster-core radial wave function (divided by r) $\chi_L(r)$ (having six interior nodes) is shown in the lower panel of Fig. 2 for $L = 0$, and since its maximum (and also the maxima of the wave functions for the higher values of L) is significantly displaced from the maximum of $V_2(r)$, we can see that γ_L will be a fairly small quantity. In fact, numerical integration of Eq. (4.9) yields values of γ_L which range from -0.23 to -0.41 as L increases from 0 to 12. These values are about a factor of 10 smaller than the equivalent quantities calculated for the $^{14}\mathrm{N}$-α system (Table 2 of Ref. 8), reflecting the very small quadrupole moment of $^{38}\mathrm{K}$.

The calculated energies of the lowest lying alpha cluster states in $^{42}\mathrm{Sc}$ (up to $L = 4$) are listed in Table III, but in view of the smallness of γ_L the main point to note is that the splittings are also not very large. The conclusion, therefore, is that the degeneracy of the L centroids is only weakly broken. Improved gamma ray spectroscopy and/or alpha transfer reactions to detect these states would be most welcome.

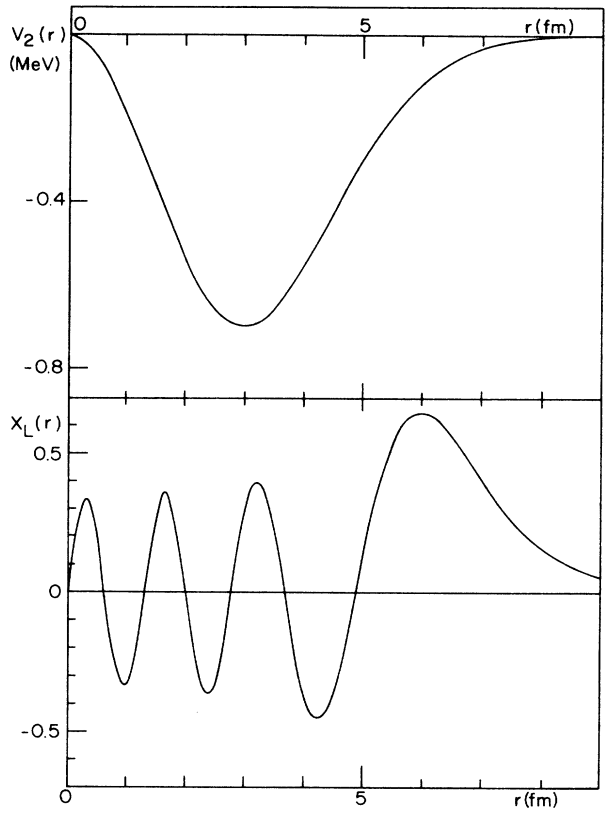

FIG. 2. Upper panel: the semimicroscopically calculated tensor form factor $V_2(r)$ in MeV for the $^{38}\mathrm{K}$-α interaction plotted as a function of the cluster-core separation distance r in fm. Lower panel: the radial wave function (divided by r) for the $L = 0$ member of the $N = 12$ band of $^{38}\mathrm{K}$-α cluster states in $^{42}\mathrm{Sc}$, also as a function of r in fm.

V. CONCLUSIONS

The Buck-Dover-Vary local potential cluster model gives an excellent description of the low lying bands of alpha particle cluster states in the nuclei at the beginning of the *sd* shell (mass numbers $16 \leq A \leq 20$). It has been applied in this paper to the $N = 12$ bands of alpha particle cluster states in the highly analogous situation at the beginning of the *fp* shell (mass numbers $40 \leq A \leq 44$). Unfortunately, a thorough evaluation of its efficacy in this region is hampered by the scarcity of experimental data (alpha particle transfer reactions and gamma ray spectroscopy) in some of these nuclei. However, in those cases where measurements are copious ($^{40}\mathrm{Ca}$, $^{44}\mathrm{Ti}$, and, to a lesser extent, $^{43}\mathrm{Sc}$) the model is very successful in reproducing excitation energies and $E2$

TABLE III. The semimicroscopically predicted energies of the lowest lying members of the $N = 12$ band of isospin-0 alpha particle cluster states in $^{42}\mathrm{Sc}$.

J^π	L	E (MeV)	J^π	L	E (MeV)
3^+	0	2.18	5^+	4	3.44
4^+	2	2.20	6^+	4	3.62
3^+	2	2.34	4^+	4	3.65
2^+	2	2.91	3^+	4	4.06
5^+	2	3.05	7^+	4	4.42
1^+	2	3.52	2^+	4	4.50
			1^+	4	4.86

transition strengths. In addition, there are enough data available for ^{42}Ca and ^{42}Sc to strongly hint that regular bands of alpha cluster states are also present there, and that they therefore persist across the entire mass range under consideration.

Original calculations of the energies and matrix elements of r^2 (the cluster-core separation distance) for the $^{42}\text{Ca}=^{38}\text{Ar}+\alpha$ and $^{42}\text{Sc}=^{38}\text{K}+\alpha$ systems are presented, and in the latter case a semimicroscopic calculation of the tensor force which lifts the degeneracy of the L centroids is performed. Although higher lying $N=13$ negative parity bands of alpha cluster states are predicted by the model in all of the *fp*-shell nuclei investigated, they are not presented here because of the complete absence of experimental measurements for comparison. It is hoped that these calculations will spur further experimental investigations of these nuclei, where there is certainly room for improved spectroscopy.

Finally, we note that the observed $L=10$ and/or 12 members of the $N=12$ alpha cluster state bands in ^{40}Ca and ^{44}Ti are lower in energy than predicted. This discrepancy could well be a result of the centrifugal antistretching effect, which leads to the average cluster-core separation becoming reduced so much that the two bodies overlap significantly for these L values, hence invalidating our simple treatment of the Pauli principle. In view of this shortcoming, we conclude that the Buck-Dover-Vary local potential cluster model can be profitably applied at the beginning of the *fp* shell, but that it is not as successful there as at the beginning of the *sd* shell. Further experimental investigations of these nuclei are clearly warranted.

[1]D. A. Bromley, in *Proceedings of the 4th International Conference on Clustering Aspects of Nuclear Structure and Nuclear Reactions,* Chester, U.K., 1984, edited by J. S. Lilley and M. A. Nagarajan (Reidel, Dordrecht, 1985), p. 1.
[2]H. J. Daley and M. A. Nagarajan, Phys. Lett. **166B**, 379 (1986).
[3]H. J. Daley and B. R. Barrett, Nucl. Phys. **A449**, 256 (1986).
[4]B. Buck, C. B. Dover, and J. P. Vary, Phys. Rev. C **11**, 1803 (1975).
[5]B. Buck, H. Friedrich, and A. A. Pilt, Nucl. Phys. **A290**, 205 (1977).
[6]B. Buck and A. A. Pilt, Nucl. Phys. **A280**, 133 (1977).
[7]B. Buck and A. A. Pilt, Nucl. Phys. **A295**, 1 (1978).
[8]B. Buck, A. C. Merchant, and N. Rowley, Nucl. Phys. **A327**, 29 (1979).
[9]A. C. Merchant, Nucl. Phys. **A417**, 109 (1984).
[10]R. A. Baldock, B. Buck, and J. A. Rubbio, Nucl. Phys. **A426**, 222 (1984).
[11]A. A. Pilt, Phys. Lett. **73B**, 274 (1978).
[12]K. F. Pal and R. G. Lovas, Phys. Lett. **96B**, 19 (1980).
[13]A. C. Merchant, J. Phys. G **10**, 885 (1984).
[14]F. Michel, G. Reidemeister, and S. Okhubo, Phys. Rev. Lett. **57**, 1215 (1986).
[15]A. C. Merchant, submitted to Phys. Rev. C.
[16]H. W. Fulbright, C. L. Bennett, R. A. Lindgren, R. G. Markham, S. C. McGuire, G. C. Morrison, U. Strohbusch, and J. Toke, Nucl. Phys. **A284**, 329 (1977).
[17]H. T. Fortune, M. N. Al-Jadir, R. R. Betts, J. N. Bishop, and R. Middleton, Phys. Rev. C **19**, 756 (1979).
[18]P. Braun-Munzinger, C. K. Gelbke, N. Grama, H. Homeyer, E. Ridinger, and R. Stock, Phys. Rev. Lett. **29**, 1261 (1972).
[19]P. M. Endt and C. van der Leun, At. Data Nucl. Data Tables **13**, 67 (1974); Nucl. Phys. **A310**, 1 (1979).
[20]H. Furutani, H. Kanada, T. Kaneko, S. Nagata, H. Nishioka, S. Okabe, S. Saito, T. Sakuda, and M. Seya, Prog. Theor. Phys. **68**, 193 (1980).
[21]F. Ajzenberg-Selove, Nucl. Phys. **A392**, 1 (1983).
[22]F. Ajzenberg-Selove, Nucl. Phys. **A460**, 1 (1986).
[23]J. B. McGrory, Phys. Rev. C **8**, 693 (1973).
[24]C. J. Batty, E. Friedman, and D. F. Jackson, Nucl. Phys. **A175**, 1 (1971); C. J. Batty and E. Friedman, Phys. Lett. **34B**, 7 (1971).